[CANCER RESEARCH 64, 4621–4628, July 1, 2004]

BPR0L075, a Novel Synthetic Indole Compound with Antimitotic Activity in Human Cancer Cells, Exerts Effective Antitumoral Activity *in Vivo*

Ching-Chuan Kuo,[1] Hsing-Pang Hsieh,[2] Wen-Yu Pan,[1] Ching-Ping Chen,[2] Jing-Ping Liou,[2] Shiow-Ju Lee,[2] Yi-Ling Chang,[2] Li-Tzong Chen,[1] Chiung-Tong Chen,[2] and Jang-Yang Chang[1]

Divisions of [1]Cancer Research and [2]Biotechnology and Pharmaceutical Research, National Health Research Institutes, Taipei, Taiwan, ROC

ABSTRACT

BPR0L075 is a novel synthetic compound discovered through research to identify new microtubule inhibitors. BPR0L075 inhibits tubulin polymerization through binding to the colchicine-binding site of tubulin. Cytotoxic activity of BPR0L075 in a variety of human tumor cell lines has been ascertained, with IC_{50} values in single-digit nanomolar ranges. As determined by flow cytometry, human cervical carcinoma KB cells are arrested in G_2-M phases in a time-dependent manner before cell death occurs. Terminal deoxynucleotidyl transferase-mediated nick end labeling assay indicates that cell death proceeds through an apoptotic pathway. Additional studies indicate that the effect of BPR0L075 on cell cycle arrest is associated with an increase in cyclin B1 levels and a mobility shift of Cdc2 and Cdc25C. The changes in Cdc2 and Cdc25C coincide with the appearance of phosphoepitopes recognized by a marker of mitosis, MPM-2. Furthermore, phosphorylated forms of Bcl-2, perturbed mitochondrial membrane potential, and activation of the caspase-3 cascade may be involved in BPR0L075-induced apoptosis. Notably, several KB-derived multidrug-resistant cell lines overexpressing P-gp170/MDR and MRP are resistant to vincristine, paclitaxel, and colchicine but not to BPR0L075. Moreover, BPR0L075 shows potent activity against the growth of xenograft tumors of the gastric carcinoma MKN-45, human cervical carcinoma KB, and KB-derived P-gp170/MDR-overexpressing KB-VIN10 cells at i.v. doses of 50 mg/kg in nude mice. These findings indicate BPR0L075 is a promising anticancer compound with antimitotic activity that has potential for management of various malignancies, particularly for patients with drug resistance.

INTRODUCTION

Microtubules are hollow tubes consisting of α- and β-tubulin heterodimers that polymerize parallel to a cylindrical axis (1). Microtubules are critical elements in a variety of fundamental cell functions, including sustained shape, transportation of vesicles and protein complexes, and regulation of motility and cell division (2). During mitosis, microtubules are at their highest dynamic instability during spindle formation and separation of chromosomes. Because microtubules play crucial roles in the regulation of the mitotic apparatus, disruption of microtubules can induce cell cycle arrest in M phase, formation of abnormal mitotic spindles, and final triggering of signals for apoptosis (3).

The discovery that the cytotoxic activity of various compounds is through interference with the mitotic spindle apparatus has attracted much attention within the past 2 decades, and microtubules have become an attractive pharmacologic target for anticancer drug discovery (4, 5). Microtubule inhibitors interfere with the dynamics of tubulin polymerization and depolymerization, which results in the inhibition of chromosome segregation in mitosis and consequently the inhibition of cell division (4). The well-characterized clinically used microtubule inhibitors are the taxanes and the *Vinca* alkaloids. Taxanes, such as paclitaxel and docetaxel, are newer antimitotic agents that stabilize microtubules and induce a net polymerization. The established class of *Vinca* alkaloids, such as vincristine, vinblastine, and vinorelbine, bind to the tubulin dimer, block the formation of new microtubules, and lead to the depolymerization of existing microtubules (4).

Although the taxanes and *Vinca* alkaloids are effective for the management of different malignancies, their potential is limited by the development of multidrug resistance (MDR) (6). MDR is multifactorial, with one pathway leading to resistance mediated by overexpression of transmembrane efflux pumps, namely, the M_r 170,000 P-glycoprotein (P-gp170/MDR) and the multidrug resistance protein (MRP; Ref. 7). These efflux pumps are able to reduce the intracellular concentrations of taxanes and *Vinca* alkaloids to a nontoxic level. Therefore, there has been great interest in identifying novel microtubule inhibitors that overcome various modes of resistance and have improved pharmacology profiles.

Combretastatin A-4 (CA-4), a naturally occurring stilbene derived from the South African tree *Combretum caffrum*, inhibits tubulin polymerization by binding to tubulin at the colchicine-binding site (8). It shows potent cytotoxicity against a broad spectrum of human cancer cell lines, including those of MDR-positive lines (9). CA-4P (disodium combretastatin-A-4–3-*O*-phosphate), a water-soluble prodrug, is a novel antitumor vascular targeting agent and is the first combretastatin analog to enter clinic trials (10, 11). Our previous work showed that 2-aminobenzophenone types of CA-4 analogs exhibited strong cytotoxic activity against a wide variety of human cancer cells, including MDR-positive cancer cells (12).

Our current work continues efforts to design and synthesize a series of 3-aroylindole compounds as novel heterocyclic CA-4 analogs and to evaluate their biological activities for further drug development (13). Among hundreds of 3-aroylindole synthetic compounds with various substituents on the indole ring, 6-methoxy-3-(3′,4′,5′-trimethoxy-benzoyl)-1H-indole (BPR0L075; Fig. 1) was identified as a potential lead based on extremely potent cytotoxicity with good pharmacologic properties. Herein, we describe the detailed molecular mechanism of action of BPR0L075 and examine whether its efficacy is affected by MDR status in selected cancer cell lines. Moreover, *in vivo* antitumor activities against human xenografts have been evaluated in murine preclinical models.

MATERIALS AND METHODS

BPR0L075. The compound BPR0L075 was synthesized at the Division of Biotechnology and Pharmaceutical Research, National Health Research Institutes, Taipei, Taiwan, ROC. BPR0L075 as a white solid was obtained in 72% yield from 6-methoxyindole and 3,4,5-trimethoxybenzoyl chloride. The detailed synthetic method will be published elsewhere.

Reagents. Colchicine, vincristine, and paclitaxel were purchased from Sigma Chemical Co. (St. Louis, MO). Polyclonal antibody to Cdc25C, monoclonal antibodies to Bcl-2, Cdc2, cyclin B1, and horseradish peroxidase-

Received 11/6/03; revised 3/15/04; accepted 4/23/04.

Grant support: Grants 92A1-CAPP06-1 and BP-092-PP10 from the National Health Research Institutes, Taiwan, ROC.

The costs of publication of this article were defrayed in part by the payment of page charges. This article must therefore be hereby marked *advertisement* in accordance with 18 U.S.C. Section 1734 solely to indicate this fact.

Requests for reprints: Jang-Yang Chang, Cancer Cooperative Ward in National Taiwan University Hospital, Division of Cancer Research, National Health Research Institutes, 7 Chung-Shan South Road, Taipei 100, Taiwan, ROC. Phone: 886-2-2356-2879; Fax: 886-2-2389-2737; E-mail: jychang@nhri.org.tw; Chiung-Tong Chen, Division of Biotechnology and Pharmaceutical Research, National Health Research Institutes, 9F, 161, Sec. 6, Minchiuan East Road, Taipei 114, Taiwan, ROC. Phone: 886-2-2653-440-ext. 6587; Fax: 886-2-2792-9703; E-mail: ctchen@nhri.org.tw.

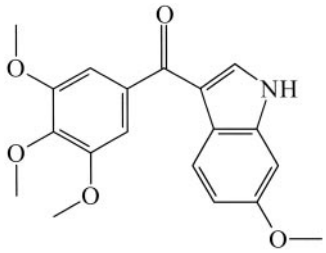

Fig. 1. Chemical structure of 6-methoxy-3-(3′,4′,5′-trimethoxy-benzoyl)-1H-indole.

conjugated secondary antibody were purchased from Santa Cruz Biotechnology (Santa Cruz, CA). Phosphospecific monoclonal antibody for MPM-2 was purchased from Upstate Biotechnology (Lake Placid, NY). Monoclonal antibody for α-tubulin was purchased from Sigma Chemical. FITC-conjugated secondary antibody was purchased from Ancell Corporation (Bayport, MN). Cell culture reagents were obtained from Life Technologies, Inc. (Rockville, MD). Microtubule-associated protein-rich tubulin and biotin-labeled tubulin were purchased from Cytoskeleton, Inc. (Denver, CO). [^{3}H]colchicine (specific activity, 60–87 Ci/mmol) and Western blot chemilluminescent reagent were purchased from Perkin-Elmer Life Sciences (Boston, MA). [^{3}H]paclitaxel (specific activity, 7.0 Ci/mmol) was purchased from Moravek Biochemicals (Brea, CA). [^{3}H]vinblastine sulfate (specific activity, 4.6 Ci/mmol) and streptavidin-labeled poly(vinyl toluene) scintillation proximity assay (SPA) beads were purchased from Amersham Pharmacia Biotech (Piscataway, NJ). 3,3′-Dihexyloxacarbocyanine iodide ($DiOC_6$) was purchased from Molecular Probes (Eugene, OR). All of the other chemicals were from E. Merck Co. (Darmstadt, Germany) or Sigma Chemical, and they were standard analytic grade or higher.

Cell Culture. Human cervical carcinoma KB cells (this cell line was originally believed to be derived from an epidermal carcinoma of the mouth but has now been shown with HeLa characteristics), nasopharyngeal carcinoma HONE-1 cells, colorectal carcinoma HT29 cells, gastric MKN-45 carcinoma cells, and glioblastoma multiforme DBTRG cells were maintained in RPMI 1640 medium supplied with 5% fetal bovine serum. Human breast carcinoma MCF-7 cells, stomach carcinoma TSGH cells, and hepatocellular carcinoma Hep G2 cells were maintained in MEM supplied with 5% fetal bovine serum. Human leukemia CEM cells were maintained in RPMI 1640 medium supplied with 20% fetal bovine serum. Human Detroit 551 fibroblasts were maintained in MEM supplied with 10% fetal bovine serum. KB-derived MDR-positive cell lines (*e.g.*, KB-VIN10, KB-TAX50, and KB-7D) were maintained in growth medium supplemented with 10 nM vincristine, 50 nM paclitaxel, and 7 μM VP-16, respectively. KB-VIN10 and KB-TAX50 cells were generated by vincristine- and paclitaxel-driven selection, respectively, and displayed overexpression of P-gp170/MDR.[3] KB-7D cells were generated by VP-16-driven selection, which displayed down-regulation of Top II and overexpression of MRP (14, 15).

Growth Inhibition Assay. Cells in logarithmic growth phase were cultured at a density of 5000 cells/ml/well in a 24-well plate. Drug-resistant cells were cultured in drug-free medium for 3 days before use. The cells were exposed to various concentrations of the test drugs for 72 h. The methylene blue dye assay was used to evaluate the effect of test drugs on cell growth, as has been described previously (16). The IC_{50} value resulting from 50% inhibition of cell growth was calculated graphically as a comparison with control growth.

Tubulin Competition-Binding SPA. The colchicine, paclitaxel, and vinblastine competition-binding SPAs were conducted as described previously using biotin-labeled tubulin and streptavidin-labeled poly(vinyl toluene) SPA beads (17–19). Briefly, radiolabeled colchicine, paclitaxel, or vinblastine sulfate (final concentration, 0.08 μM, 0.16 μM, or 0.25 μM, respectively), unlabeled compound, and special long-chain biotin-labeled tubulin (0.5 μg for colchicines and paclitaxel tubulin competition-binding SPA, and 1.0 μg for vinblastine tubulin competition-binding SPA) were incubated together in 100 μl binding buffer [80 mM PIPES (pH 6.8), 1 mM EGTA, 10% glycerol, 1 mM $MgCl_2$, and 1 mM GTP] for 2 h at 37°C. Streptavidin-labeled SPA beads (80 μg, 160 μg, or 200 μg that suspended in 25 μl binding buffer) were added to each reaction mixture for colchicine, paclitaxel, or vinblastine assay, respectively. The inhibition constant (K_i) was calculated using the Cheng-Prusoff equation (20).

***In Vitro* Microtubule Assembly Assay.** The assay was basically performed according to Bollag *et al.* (21). In brief, microtubule-associated protein-rich tubulin in 100 μl buffer containing 100 mM PIPES (pH 6.9), 2 mM $MgCl_2$, 1 mM GTP, and 2% (v/v) DMSO was placed in 96-well microtiter plates in the presence of test agents. The increase in absorbance was measured at 350 nm in a PowerWave X Microplate Reader (Bio-Tek Instruments, Winooski, VT) at 37°C and recorded every 30 s for 30 min. The area under the curve was used to determine the concentration that inhibited tubulin polymerization by 50% (IC_{50}). The area under the curve of the untreated control was set to 100% polymerization, and the IC_{50} was calculated by nonlinear regression.

***In Vivo* Microtubule Assembly Assay.** Separation of insoluble polymerized microtubules from soluble tubulin dimers and analysis of the effect of various antimitotic agents on tubulin polymerization *in vivo* were performed as described by Blagosklommy *et al.* (22). In brief, KB and KB-VIN10 cells at a density of 1×10^6/100-mm^2 dishes were treated with indicated concentrations of test agents for the selected treatment duration. Cells then were washed with PBS three times before adding lysis buffer containing 20 mM Tris-HCl (pH 6.8), 1 mM $MgCl_2$, 2 mM EGTA, 20 μg/ml aprotinin, 20 μg/ml leupeptin, 1 mM phenylmethylsulfonyl fluoride, 1 mM orthovanadate, and 0.5% Nonidet. Supernatants were collected after centrifugation at 15,000 $\times$ *g* for 10 min at 4°C. The pellets were dissolved in an SDS-PAGE sampling loading buffer and heated at 95°C for 10 min to dissolve the pellets; the resulting material was subjected to electrophoresis on 10% SDS-polyacrylamide gels. After electrophoresis, the proteins were transferred to a nitrocellulose membrane, and the membrane was blocked with 5% skim milk/PBS-Tween 20 overnight at 4°C. The relative amounts of tubulins were detected by anti-α-tubulin monoclonal antibody and horseradish peroxidase-conjugated secondary antibody. Detection of immunoreactive signal was accomplished with Western blot chemilluminescent reagent.

Immunocytochemistry. KB and KB-VIN10 cells plated on coverslips were treated with indicated concentration of test agents for the selected treatment duration. After treatment, cells were placed in the fixation solution (methanol:acetone = 1:1, v/v) for 1 h at −20°C and washed with PBS. Cells then were blocked with 5% skim milk in PBS for 1 h before further incubation with 5% skim milk in PBS containing anti-α-tubulin monoclonal antibody for 2 h at room temperature. After being washed with PBS, cells were reincubated with FITC-conjugated secondary antibody in the dark room for 1 h. Cellular microtubules were observed with an Olympus BX50 fluorescence microscope (Dulles, VA).

Analysis of Cell Cycle Distribution. Cells were initially seeded at 1×10^6 cells in 100-mm^2 dishes and then incubated in various concentrations of BPR0L075 for the indicated time. Adherent and floating cells after pooling then were collected, washed once in PBS, and resuspended in 200 μl of PBS. Cells then were added drop-wise to 5 ml ice-cold 70% ethanol with vortexing and stored at −20°C until analysis. Fixed cells were collected by centrifugation; washed twice with PBS; resuspended in 1 ml of a solution containing 3.4 mM sodium citrate, 20 μg/ml propidium iodide, and 100 μg/ml RNase A; and stored in the dark for 1 h. Cells were analyzed using a FACSVantage flow cytometer (Becton Dickinson, Franklin Lakes, NJ). Cell cycle analysis was performed according to the mathematical model of Jett (23).

Western Blot Analysis for Bcl-2 and G_2-M Regulatory Proteins. Cells were initially seeded at a density of 1×10^6 in 100-mm^2 dishes. After treatment for the indicated time with various concentrations of BPR0L075, adherent cells were washed twice with PBS, gently scraped from the dishes, centrifuged, lysed in ice-cold lysis buffer [50 mM Tris (pH 7.4), 0.8 M NaCl, 5 mM $MgCl_2$, 0.5% NP40, 1 mM phenylmethylsulfonyl fluoride, 1 μg/ml pepstatin, and 50 μg/ml leupeptin], and cleared by microcentrifugation. Total cell lysates (50 μg/well) were separated by SDS-PAGE and electrophoretically transferred onto nitrocellulose membranes. Membranes were blocked with 5% skim milk/PBS-Tween 20 overnight at 4°C and probed with appropriate dilutions (as recommended by the manufacturers) of primary antibody for 1 h at room temperature. Membranes then were washed three times in PBS-Tween 20 and subsequently incubated with appropriate horseradish peroxidase-conjugated secondary antibody for 1 h at room temperature. After washing,

[3] Unpublished observations.

immunoreactive proteins were visualized using Western blot chemilluminescent reagent.

Evaluation of the Mitochondrial Transmembrane Potential. The ampholytic cationic fluorescent probe $DiOC_6$ was used to monitor drug-induced changes in the mitochondrial transmembrane potential ($\Delta\Psi_m$; Ref. 24). Briefly, cells were initially seeded at 1×10^6 cells in 10-mm^2 dishes and then treated with various concentrations of BPR0L075 for 24 h. After drug treatment, cells were loaded with the probe $DiOC_6$ (40 nM) for 30 min at 37°C before cytometric analysis. The supernatant was removed, and the cells were harvested and resuspended in PBS. Measurement of the retained $DiOC_6$ in 10,000 cells of each sample was performed in a FACSVantage flow cytometer (Becton Dickinson). $DiOC_6$ was excited at 488 nm, and fluorescence was analyzed at 525 nm (FL-1) after logarithmic amplification.

Determination of Caspase-3 Activity. Caspase-3 activity was measured with use of the CaspACE Assay System Fluorometric Kit (Promega Corporation, Madison, WI). Cells were initially seeded at a density of 1×10^6 in 100-mm^2 dishes. After treatment for the indicated time with various concentrations of BPR0L075, caspase-3 activity was measured by the cleavage of the fluorometric substrate Ac-DEVD-AMC according to manufacturer's instructions.

TUNEL Assay. To determine whether BPR0L075 could induce apoptosis, terminal deoxynucleotidyl transferase-mediated nick end labeling (TUNEL) assay with *In Situ* Cell Death Detection Kit-Fluorescein (Roche Molecular Biochemicals, Mannheim, Germany) was performed. Cells treated with various concentrations of BPR0L075 for 24 h at 37°C were subjected to an assay kit according to the manufacturer's instructions.

Animals and s.c. Implantation of Cancer Cells. The implantation of cancer cells was carried out similarly to previous reports with modification (25). Male Ncr and CD1 nude mice (5–6-weeks-old) were purchased from Taconic (Germantown, NY) and Charles River Laboratories (Wilmington, MA), respectively. The animals were housed and the experiments were carried out at an International Association for Assessment and Accreditation of Laboratory Animal Care-accredited animal facility of the Developmental Center for Biotechnology, Taipei, Taiwan. The Institutional Animal Care and Use Committees for Biotechnology and the National Health Research Institutes approved uses of animals in these studies.

The animals were s.c. implanted with 5×10^5 MKN-4, 1×10^6 KB cells, or 1×10^6 KB-VIN10 mixed with equal volume of Matrigel (Becton Dickinson) in 0.1 ml at one flank per mouse via a 22-gauge needle. Tumor growth was examined twice a week after implantation, and the volume of tumor mass was measured with an electronic caliper and calculated as $1/2 \times \text{length} \times \text{width}^2$ in mm^3.

Drug Treatments and Monitoring of *in Vivo* Antitumoral Activity. BPR0L075 was dissolved completely in a vehicle mixture of DMSO/cremophor/saline (1:4:15). In MKN-45 and KB xenograft studies, when the size of a growing tumor reached ≥100 mm^3, the xenograft tumor-bearing nude mice were treated with BPR0L075 i.v. via the tail veins at 10, 25, or 50 mg/kg for 5 days/week for 2 consecutive weeks or 50 mg/kg daily for the entire period of observation. In KB-derived P-gp170/MDR-overexpressing KB-VIN10 xenograft study, mice were treated with BPR0L075 at 50 mg/kg for 5 days/week for 2 consecutive weeks. Vincristine was included for comparisons and was administered at a dose regimen close to its maximal tolerated dose of 1 mg/kg at 1 dose/week for 2 weeks in mice. The control group was treated with vehicle mixture only. Tumor size and animal body weight were measured twice a week after drug treatment. At the end of the experiments, animals were euthanized with carbon dioxide inhalation, followed by cervical dislocation. Data were statistically analyzed, and significant differences between testing groups were determined by ANOVA ($P < 0.05$).

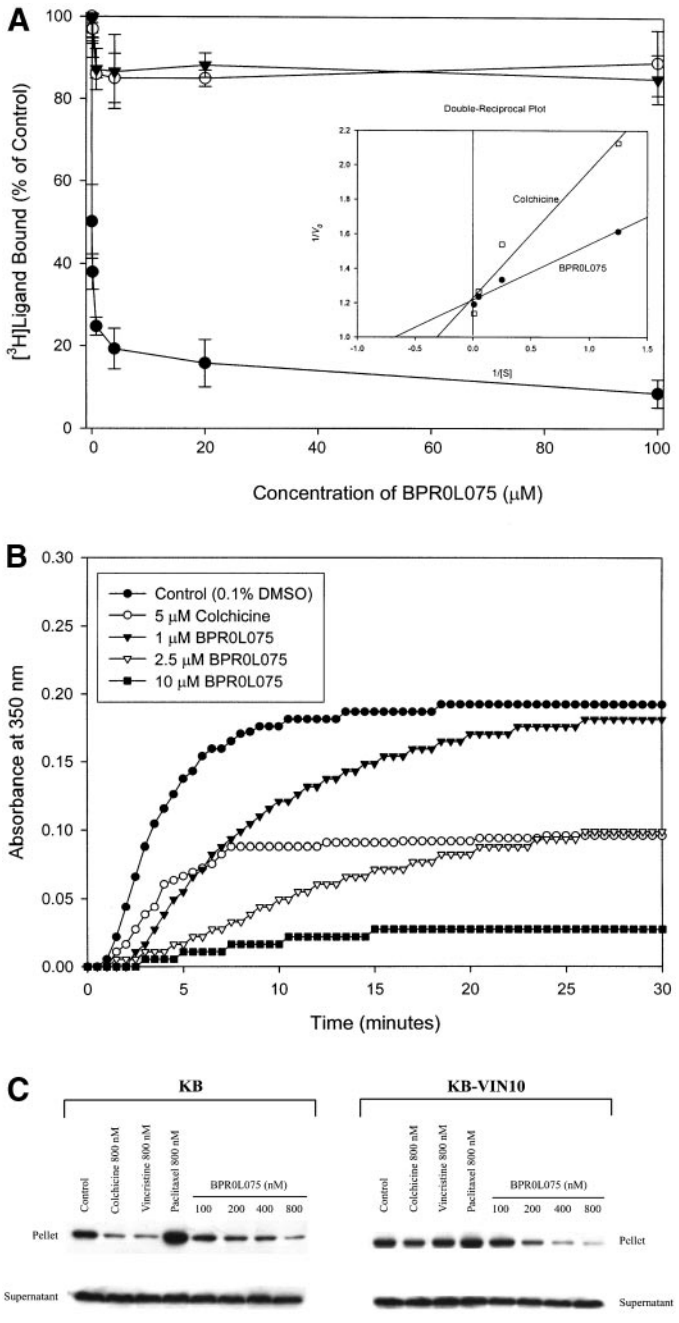

Fig. 2. 6-Methoxy-3-(3′,4′,5′-trimethoxy-benzoyl)-1H-indole (*BPR0L075*) binds to the colchicine-binding site of tubulin and inhibits microtubule polymerization. *A*, [^{3}H] ligands bound curve. Tubulin was incubated with the radiolabeled ligand at 37°C, and the amount of radioligand bound was determined by using scintillation proximity assay beads. [^{3}H]colchicine (●), [^{3}H]paclitaxel (○), and [^{3}H]vinblastine (▼) competition-binding curves, respectively. *Each data point*, the mean ± SD. Double-reciprocal plot showed that BPR0L075 is a competitive inhibitor of colchicine binding to tubulin, colchicine (□), and BPR0L075 (●) (*insert*). *B*, BPR0L075 inhibits microtubule assembly *in vitro*. Purified tubulin protein in a reaction buffer was incubated at 37°C in the absence (control, ●) or presence of colchicine (5 μM, ○), BPR0L075 (1 μM, ▼; 2.5 μM, ▽; and 10 μM, ■). *C*, BPR0L075 inhibits microtubule assembly *in vivo*. KB and KB-VIN10 cells were treated with test agents or with the same volume of DMSO in PBS as control. After 6-h incubation, cells were lysed in lysis buffer. Cell lysates were centrifuged to separate polymerized microtubules from tubulin dimers as described in "Materials and Methods." After gel electrophoresis and transfer to nitrocellulose membrane, α-tubulin was visualized by Western blot analysis.

RESULTS

Growth Inhibition of BPR0L075 against Various Human Tumor Cells. Initial experiments were conducted for evaluation of growth inhibition by BPR0L075 against various human cancer cell lines. The results showed that BPR0L075 inhibited the growth of several human cancer cell lines from different tissues and organs, including cervical carcinoma KB cells, nasopharyngeal carcinoma HONE-1 cells, colorectal carcinoma HT29 cells, glioblastoma multiforme DBTRG cells, breast carcinoma MCF-7 cells, gastric carcinoma TSGH and MKN-45 cells, hepatoma Hep G2 cells, and leukemia CEM cells, with IC_{50} values in single-digit nanomolar ranges (data not shown). It also displayed similar or greater growth inhibitory

activities than that of CA-4 toward several human cancer cells.[3] However, the IC_{50} of BPR0L075 toward cultured fibroblast Detroit 551 was >1000 nM. This result demonstrated that BPR0L075 possessed great selectivity between normal and cancer cells.

BPR0L075 Binds to the Colchicine-Binding Site of Tubulin and Inhibits the Polymerization of Microtubules. Because BPR0L075 is a novel heterocyclic CA-4 analog, we wanted to determine whether BPR0L075 interacts directly with tubulin through binding of the colchicine-binding site. According to tubulin competition-binding SPA, we found that, for a concentration range of 0.016–100 μM, BPR0L075 competed with [^{3}H]colchicines binding to tubulin. The binding capacity of BPR0L075 to the colchicine-binding site of tubulin is stronger than that of colchicine. The K_i values for colchicine and BPR0L075 are 1.24 and 0.023 μM, respectively. However, it did not compete with either [^{3}H]paclitaxel or [^{3}H]vinblastine binding to tubulin (Fig. 2*A*). To test the effect of BPR0L075 on microtubule assembly *in vitro*, we incubated purified, unpolymerized, microtubule-associated protein-rich tubulin with various concentrations of BPR0L075 and measured polymerization. In the control sample without the addition of any test agent, absorbance at 350 nm increases with time. In the presence of 5 μM colchicine, tubulin polymerization is inhibited ~54% compared with that of a control sample after 10-min incubation. Furthermore, in the presence of BPR0L075, tubulin polymerization is inhibited in a concentration-dependent manner. The inhibitory concentration that reduces polymerized tubulin by 50% is 3.3 ± 0.5 μM (n = 3; Fig. 2*B*). In Fig. 2*C*, the effect of BPR0L075 on microtubule assembly is compared with that of paclitaxel, vincristine, and colchicine in an *in vivo* assay. After KB cells are treated with various antimitotic agents for 6 h in the presence of 800 nM colchicine and 80 nM vincristine, inhibition of microtubule assembly is observed. In contrast, 800 nM paclitaxel promotes tubulin polymerization. Similar to the effect of colchicine and vincristine, BPR0L075 inhibits tubulin polymerization in a concentration-dependent manner (Fig. 2*C*).

We further examined the effect of BPR0L075 on cellular microtubule networks by using immunofluorescence techniques. As shown in Fig. 3*A*, the microtubule network exhibits normal arrangement and organization in KB cells in the absence of drug treatment. However, after 6-h drug treatment, 500 nM of colchicine significantly causes cellular microtubule depolymerization; we noted that most cells had short microtubule fragments scattered throughout the cytoplasm. In contrast, 500 nM of paclitaxel dramatically promotes microtubule polymerization with an increase in the density of cellular microtubules and formation of long thick microtubule bundles. Furthermore, BPR0L075 treatment results in findings similar to those of colchicine-induced microtubule change. We observed an almost complete loss of microtubules with only a diffuse stain visible throughout the cytoplasm (Fig. 3*A*). In addition, KB cells treated with low concentration of BPR0L075 ranging from 5–80 nM for 24 h also significantly induce microtubule disassembly in a concentration-dependent manner (Fig. 3*B*).

BPR0L075 Is Cytotoxic toward P-gp170/MDR and MRP Tumor Cell Lines via Prevention of Tubulin Polymerization. One major mechanism of acquired drug resistance is the overexpression of efflux pumps, namely, P-gp170/MDR and MRP (7). Cell lines selected for expression of drug efflux pumps by long-term drug expo-

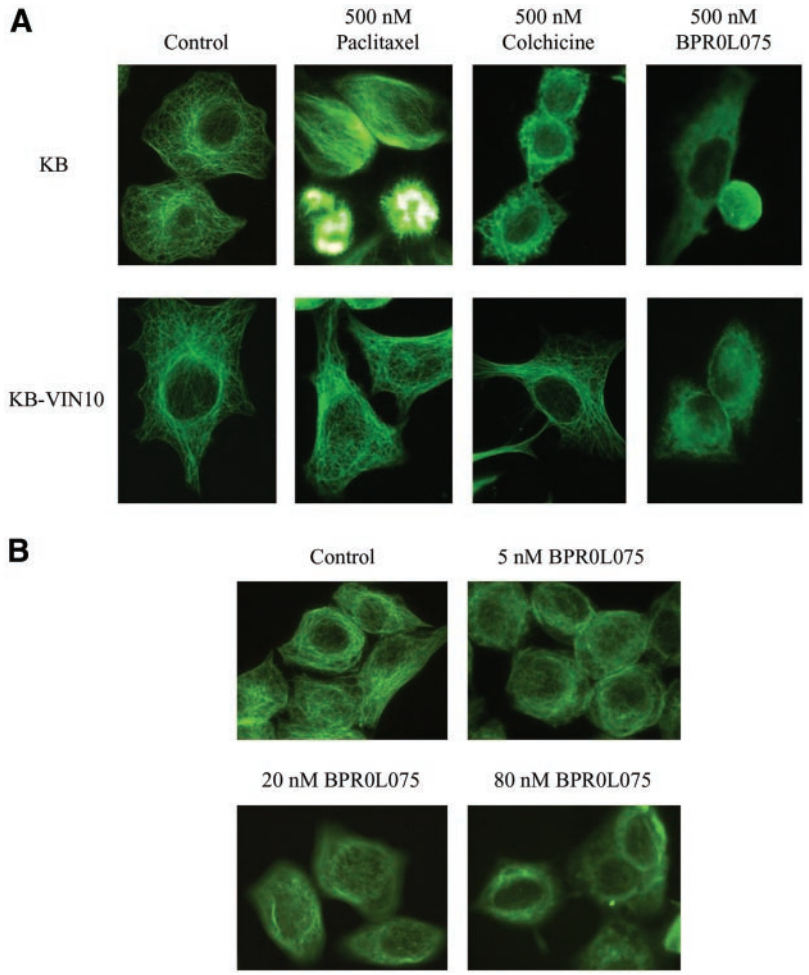

Fig. 3. Effect of 6-methoxy-3-(3′,4′,5′-trimethoxy-benzoyl)-1H-indole (*BPR0L075*) on the organizations of cellular microtubule network. *A*, KB and KB-VIN10 cells were treated with 500 nM of antimitotic agents for 6 h. *B*, KB cells were treated with BPR0L075 ranging from 5–80 nM for 24 h. After incubation, cells were harvested and fixed with fix solution. Fixed cells were reacted with monoclonal anti-α-tubulin antibody at room temperature for 2 h. After reacted with FITC-conjugated secondary antibody, the cellular microtubules were observed by Olympus-BX50 fluorescence microscope.

Table 1 *Anticancer efficacy of BPR0L075 against KB-derived MDR-positive cell lines with different resistance phenotypes*[a]

Cells were treated with various concentrations of test compounds for 72 h. Cell survival was determined by methylene blue assay. Each IC_{50} value was calculated as described in "Materials and Methods." Each value represents the mean ± SD of three independent experiments.

KB-derived cell lines	Resistance type	Growth inhibition, (IC_{50}) [nM]			
		BPR0L075	Colchicine	Vincristine	Paclitaxel
KB	(Parental)	3.6 ± 1.8	10.5 ± 2.2	0.6 ± 0.2	4.1 ± 1.6
KB-VIN10	P-gp170/MDR	2.9 ± 1.5	115 ± 7.2	90.1 ± 7.4	16,500 ± 707
KB-TAX50	P-gp170/MDR	3.1 ± 0.3	31.9 ± 2.4	1.8 ± 0.5	130 ± 6.9
KB-7D	MRP	4.2 ± 1.9	55.2 ± 7.8	1.2 ± 0.4	7.9 ± 0.5

[a] BPR0L075, 6-methoxy-3-(3′,4′,5′-trimethoxy-benzoyl)-1H-indole; MDR, multidrug resistance; MRP, multidrug resistance protein.

sure also were used to compare the antitumoral activity of BPR0L075 with that of other microtubule inhibitors. As summarized in Table 1, KB-VIN10 cells have profound resistance to paclitaxel (4024-fold), vincristine (150-fold), and colchicine (10-fold) compared with parental cells. KB-TAX50 and KB-7D cells are moderately resistant to paclitaxel, vincristine, and colchicine (2–33-fold). In contrast, BPR0L075 is equally potent toward the parental KB cells and those of KB-derived MDR-positive cell lines. The IC_{50} of BPR0L075 for a variety of KB-derived MDR-positive cells ranged from 2–4 nM.

Furthermore, we examined the microtubule polymerization status in KB-VIN10 cells compared with their parental KB cell line after 6-h treatment with colchicine, vincristine, paclitaxel, or BPR0L075. We observed an effect on microtubules after colchicine, vincristine, or paclitaxel treatment in parental KB cells but not in the KB-VIN10 cells that overexpress P-gp170/MDR (Fig. 2*C*). However, BPR0L075 still can inhibit microtubule assembly in a concentration-dependent manner in KB-VIN10 cells (Fig. 2*C*). Results from immunocytochemistry studies also demonstrate that changes on the microtubule network are not observed after colchicine and paclitaxel treatment in KB-VIN10 cells. However, BPRL075 treatment induces similar changes in cellular microtubule networks between KB and KB-VIN10 cells (Fig. 3*A*).

BPR0L075 Induces G_2-M Phase Arrest and Change in Expressed and Phosphorylated Status of G_2-M Regulators in KB Cells. The effect of BPR0L075 on cell cycle progression of KB cells was examined by flow cytometry. BPR0L075 treatment results in a time-dependent accumulation of KB cells in the G_2-M phase with concomitant losses from G_0-G_1 phase. No change of S-phase was observed (Fig. 4*A*). BPR0L075 treatment results in accumulation of cells in G_2-M phase starting with an 8-h exposure, with a maximum accumulation observed by 16 h. However, a characteristic hypodiploid DNA content peak (sub-G_1), indicated as apoptotic cells, can be detected with treatment duration of ≥24 h. The value of sub-G_1 phase reaches a peak at 48 h (~50%; Fig. 4*A*). These results indicate that BPR0L075-induced cells are arrested in G_2-M phase before cell death occurs.

Furthermore, we investigated the association between BPR0L075-induced G_2-M phase arrest and alteration in G_2-M regulatory protein expression. As shown in Fig. 4*B*, BPR0L075 causes a concentration-dependent increase in cyclin B1. In addition, slower migrating forms of Cdc25C protein are present in cells after 24-h treatment with BPR0L075 in a concentration-dependent manner, indicative of changes in the phosphorylation state of Cdc25C (Fig. 4*B*). In contrast, there is a shift to the faster migrating form of the cyclin-dependent kinase Cdc2, consistent with the presence of the hypophosphorylated active form of the protein (Fig. 4*B*). We further examined the status of phosphorylated polypeptides found only in mitotic cells using MPM-2 antibody. After 24-h treatment with BPR0L075, significant elevation in the levels of MPM-2 phosphoepitopes at a concentration of 20 nM is observed (Fig. 4*B*).

BPR0L075 Initiates Bcl-2 Phosphorylation, Followed by Damage to Mitochondria and Induced Apoptosis. The Bcl-2 protein located on the outer mitochondrial membrane is important for suppression of mitochondrial manifestations of apoptosis (26), and its phosphorylation is a common characteristic of antimitotics (27). We examined whether BPR0L075-induced G_2-M phase arrest and apoptosis are associated with Bcl-2 phosphorylation. As shown in Fig. 5*A*, the appearance of the characteristically slower migrating form of

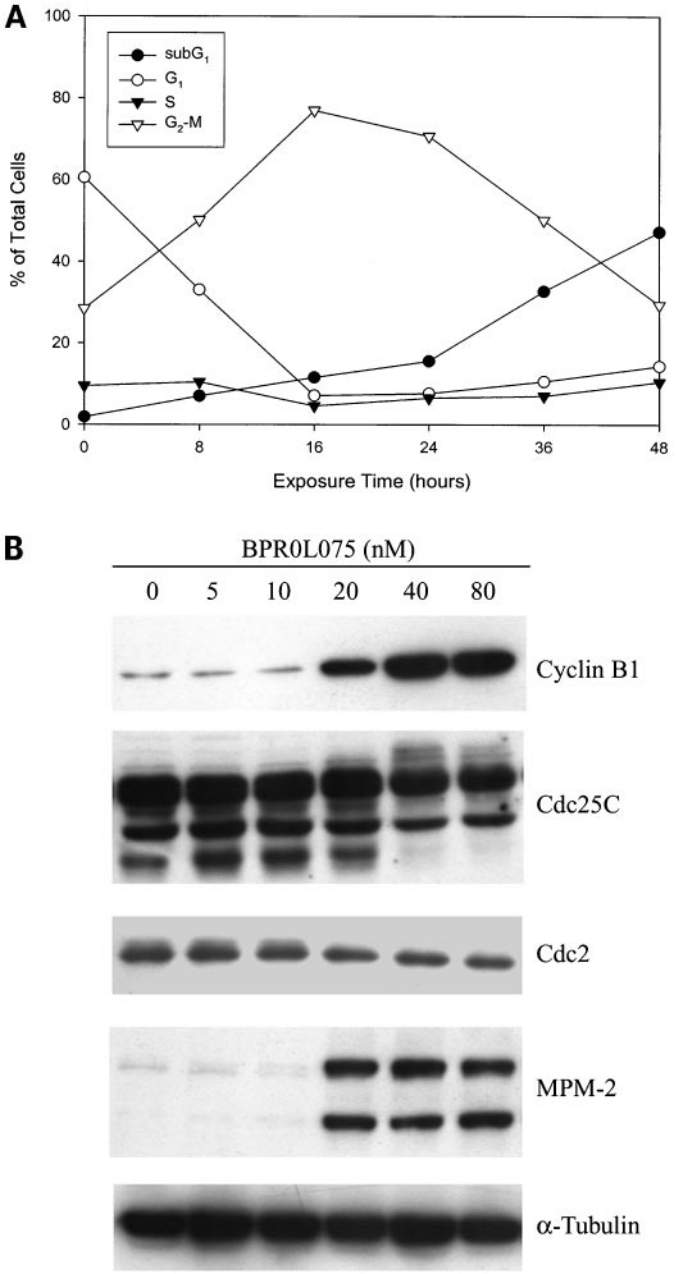

Fig. 4. 6-Methoxy-3-(3′,4′,5′-trimethoxy-benzoyl)-1H-indole (*BPR0L075*) induces G_2-M phase arrest and change in expressed and phosphorylated status of G_2-M regulators in KB cells. *A*, the time effect of BPR0L075 on cell cycle distribution in KB cells. Cells were treated with 10 nM of BPR0L075 for the indicated time and analyzed for propidium iodide-stained DNA content by flow cytometry. *B*, change in expressed and phosphorylated status of G_2-M regulators after BPR0L075 treatment. Cells were harvested after BPR0L075 treated for 24 h, and cell extract was prepared and loaded on SDS-PAGE. After electrophoresis, proteins were transferred to blots and probed with cyclin B1, Cdc25C, Cdc2, and MPM-2, as well as internal control, α-tubulin antibodies.

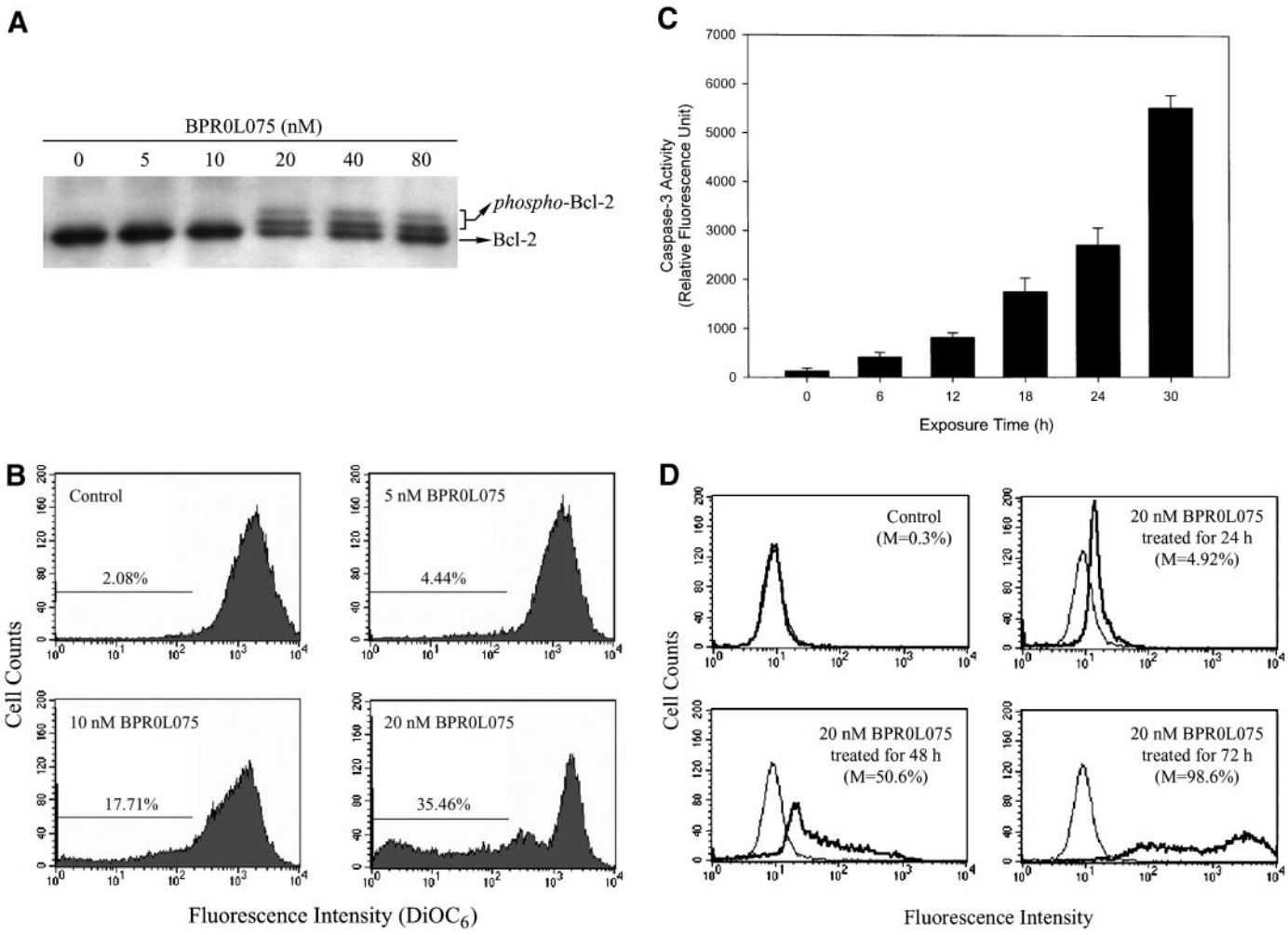

Fig. 5. 6-Methoxy-3-(3′,4′,5′-trimethoxy-benzoyl)-1H-indole (*BPR0L075*) initiates Bcl-2 phosphorylation, followed by damage to mitochondria and induced apoptosis in KB cells. *A*, BPR0L075 induces Bcl-2 phosphorylation. Cells were harvested after BPR0L075 treated for 24 h, and cell extract was prepared and loaded on SDS-PAGE. After electrophoresis, proteins were transferred on the nitrocellulose membrane, and Bcl-2 was analyzed by Western blot analysis. *B*, reduction of mitochondrial transmembrane potential by BPR0L075. KB cells were treated with various concentrations of BPR0L075. After 24 h of incubation, cells were incubated with 40 nM dihexyloxacarbocyanine iodide ($DiOC_6$), followed immediately by flow cytometry analysis. The *X* axis represents the $DiOC_6$ fluorescence. The *Y* axis represents the number of cells. The percentage of low-$DiOC_6$ fluorescence-gated cell is indicated. *C*, time-dependent increase in caspase-3 activity in KB cells after BPR0L075 treatment. Cells were treated with 60 nM of BPR0L075 for the indicated time and analyzed caspase-3 activity using the fluorogenic tetrapeptide Ac-DEVD-AMC cleavage assay. Each point represents the mean ± SD. *D*, BPR0L075-induced apoptosis was assessed by terminal deoxynucleotidyl transferase-mediated nick end labeling (TUNEL) assay. KB cells were treated with indicated concentrations of BPR0L075 for the selected treatment duration. Apoptosis was detected by TUNEL assay and as described in "Material and Methods," and the apoptotic index (*M*) is expressed as a percentage of TUNEL-positive cells.

Bcl-2, consistent with phosphorylation, is detected after treatment with up to 20 nM BPR0L075 for 24 h. Because Bcl-2 prevents the initiation of the cellular program by stabilizing mitochondrial permeability and preventing subsequent release of cytochrome *c* to prevent caspase activation, we used the ampholytic cationic fluorochrome $DiOC_6$ to monitor changes in $\Delta\Psi_m$ induced by BPR0L075 (28). As presented in Fig. 5*B*, cells treated with BPR0L075 exhibit a significant reduction in cellular uptake of the fluorochrome $DiOC_6$, indicating a loss of $\Delta\Psi_m$, in a concentration-dependent manner. The percentage of cells with reduced $DiOC_6$ fluorescence reaches 17.7% and 35.5% after treatment with 10 and 20 nM BPR0L075, respectively, for 24 h. Caspase-1 and caspase-3 are key executioners of apoptosis, and their involvement in apoptosis also was investigated in KB cells treated with BPR0L075 (29). As shown in Fig. 5*C*, incubation of KB cells with BPR0L075 results in activation of caspase-3 in a time-dependent manner, starting with a 6-h exposure (3.13-fold compared with control group) and reaching a maximum of 41.5-fold induction by 30 h of BPR0L075 treatment. In contrast, no cleavage of caspase-1 substrate was detected after BPR0L075 treatment (data not shown). To further confirm that BPR0L075 leads to apoptosis, the TUNEL assay was used to characterize DNA strand breaks *in situ* (30). As shown in Fig. 5*D*, control cells containing intact genomic DNA appear in TUNEL-positive cells at nearly undetectable levels (0.3%), whereas ~4.9%, 50.6%, and 98.6% of TUNEL-positive cells are detected within the population of cells treated with 20 nM BPR0L075 for 24, 48, or 72 h, respectively.

Efficacy of BPR0L075 in Xenograft Experiments *in Vivo*. The potential antitumoral effect of BPR0L075 *in vivo* was assessed in human tumor xenografts in mice. KB cells were grown as s.c. tumors in nude mice. Nine days afterward, when well-established KB xenografts were palpable with tumor size of ~100 mm^3, mice were randomized into vehicle control and treatment groups of seven animals each. The treated mice received 50 mg/kg of BPR0L075 i.v. for the entire period of observation (days 9–30 after cancer cell inoculation), or they received 10, 25, or 50 mg/kg of BPR0L075 for 5 days/week for 2 consecutive weeks (days 9–13 and 16–20 after inoculation). There was a dose-dependent decrease in tumor volume in mice treated with BPR0L075 5 days/week for 2 consecutive weeks. Moreover, there was an ~82% decrease in tumor volume on day 30 in the animals daily treated with 50 mg/kg/day BPR0L075 for the

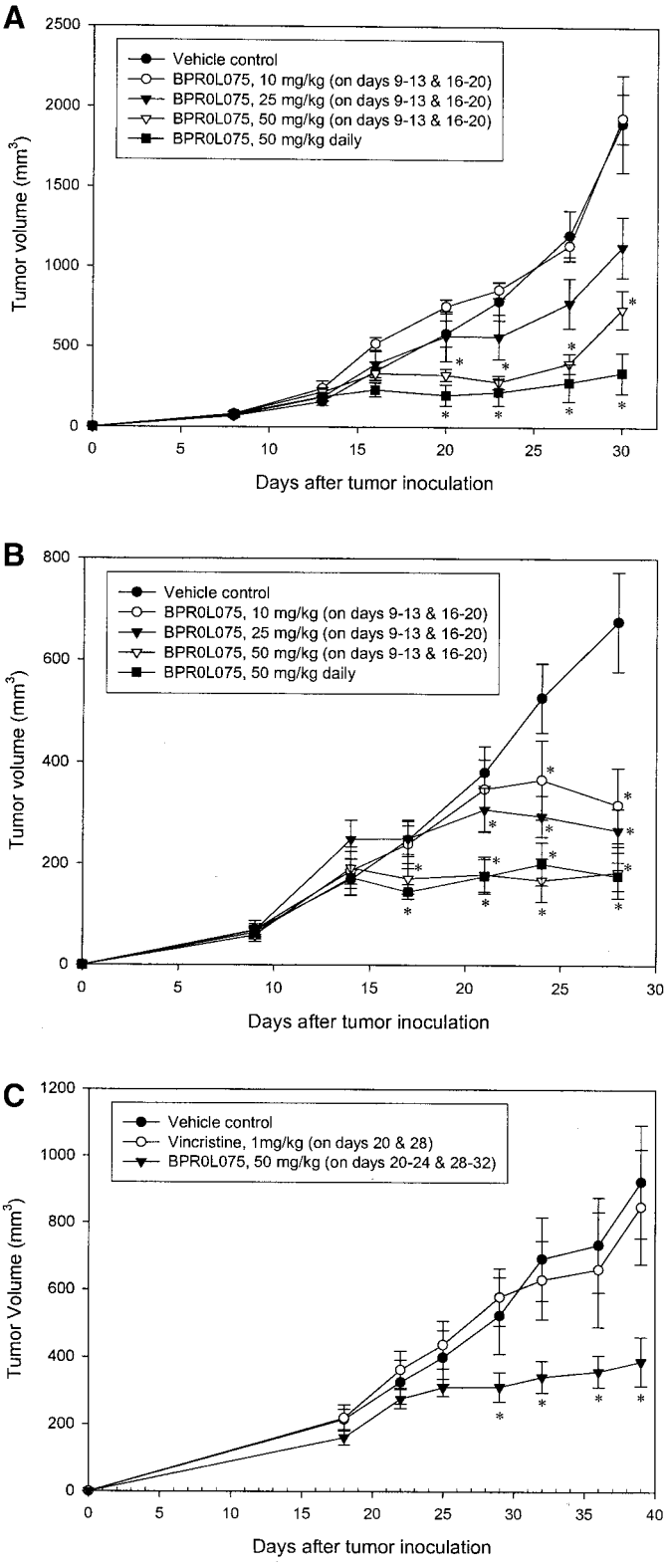

Fig. 6. Inhibition of human xenografts growth *in vivo* by 6-methoxy-3-(3′,4′,5′-trimethoxy-benzoyl)-1H-indole (*BPR0L075*). Nude mice bearing (*A*) human cervical carcinoma KB and (*B*) human gastric carcinoma MKN-45 xenografts were treated with vehicle control (●), 10 mg/kg BPR0L075 for 5 days/week for 2 weeks (on days 9–13 and 16–20; ○), 25 mg/kg BPR0L075 for 5 days/week for 2 weeks (on days 9–13 and 16–20; ▼), 50 mg/kg BPR0L075 for 5 days/week for 2 weeks (on days 9–13 and 16–20; ▽), or 50 mg/kg BPR0L075 daily for the entire period of observation (■). *C*, P-gp170/MDR-overexpressing KB-VIN10 xenograft was treated with vehicle control (●), 1 mg/kg vincristine for 1 day/week for 2 weeks (on days 20 and 28; ○), or 50 mg/kg BPR0L075 for 5 days/weeks for 2 weeks (on days 20–24 and 28–32; ▼). Data are the mean ± SD of tumor volume (mm^3) at each time point ($n = 7$; $*P < 0.05$).

entire period of observation ($P < 0.05$; Fig. 6*A*). We also used MKN-4 xenograft tumor to evaluate the efficacy of BPR0L075 against gastric tumor growth *in vivo*. Compared with tumor growth in control mice, the growth of MKN45 tumor was significantly inhibited in a dose-dependent manner in mice that received BPR0L075 treatment, with the greatest antitumoral efficacy in animals treated daily with BPR0L075 at 50 mg/kg for the entire period of observation (Fig. 6*B*). Notably, BPR0L075 also is effective toward MDR xenograft as it is in cultured MDR cells (Fig. 6*C*). BPR0L075 was well tolerated after dosing up to 50 mg/kg with no signs of toxicity in these three xenograft tumor models because loss of body weight after the treatment was <15% in all treatment groups (data not shown). Thus, BPR0L075 exerts potent antitumoral efficacy toward these three solid tumor xenografts.

DISCUSSION

BPR0L075 is a novel synthetic 3-aroylindole compound that exerts a broad spectrum of activity against human leukemia, glioblastoma, oral, nasopharyngeal, breast, gastric, colorectal, and liver cancer cells *in vitro* and strongly inhibits tubulin polymerization through binding of tubulin's colchicine-binding site (Fig. 2). Consistent with these biochemical effects, BPR0L075 disrupts intracellular microtubule network in intact cells as demonstrated in the immunocytochemistry studies (Fig. 3).

As with other microtubule-interacting agents, BPR0L075 arrests the growth of cancer cells at the G_2-M phase (Fig. 4*A*) and then induces apoptotic cell death (Fig. 5). Different classes of cyclins and their cyclin-dependent kinases control cell cycle progression. In eukaryotic cells, cyclin B and Cdc2 kinase regulate the onset of M phase. Extensive studies have shown that activation of Cdc2 kinase at the G_2-M transition requires accumulation of cyclin B and dephosphorylation of Cdc2 (31). The conversion of Cdc2 from inactive to active form is accomplished by the phosphatase Cdc25C (32, 33). Phosphorylation of Cdc25C directly stimulates its phosphatase activity, and this is necessary to activate Cdc2/cyclin B1 kinase on entry into mitosis (34). Many antimitotic drugs that interfere with normal formation of mitotic spindles either by increasing microtubule stability or by depolymerization can cause cells to arrest at the prometaphase/metaphase-to-anaphase transition known as the mitotic checkpoint (35). In this study, we demonstrate that in addition to directly disrupting microtubules, BPR0L075 treatment leads to inappropriate accumulation of cyclin B and initiates a phosphorylation cascade resulting in the engagement of active Cdc2 kinase and phosphorylation of Cdc25C (Fig. 4*B*). The changes in Cdc2 and cdc25C coincide with the appearance of phosphoepitopes recognized by a marker of mitosis, MPM-2, which is an antibody that recognizes phosphorylated polypeptides found only in mitotic cells (Ref. 36; Fig. 4*B*). These changes in protein phosphorylation are consistent with cell cycle arrest in mitosis (37).

Apoptosis induced by antimitotic agents has been associated with alterations in a variety of cellular signaling pathways. It is known that Bcl-2 is a guardian of microtubule integrity (27). Microtubule inhibitors such as vincristine, vinblastine, colchicine, paclitaxel, and doxetaxel induce growth arrest, followed by phosphorylation and inactivation of Bcl-2, and eventually leading to apoptotic cell death in the G_2-M phase of the cell cycle (3, 18, 38–40). As with other microtubule-damaging agents, BPR0L075 also is able to induce Bcl-2 hyperphosphorylation in a concentration-dependent manner (Fig. 5*A*). The mechanism by which Bcl-2 opposes apoptosis may involve prevention of mitochondrial damage (*e.g.*, loss of $\Delta\Psi_m$; Refs. 41, 42). The collapse of $\Delta\Psi_m$ results in an uncoupling of the respiratory chain and the efflux of small molecules (*e.g.*, cytochrome *c* and calcium) and

certain proteins (including caspase-2 and caspase-9; Ref. 43), as well as the apoptosis-inducing factor that can, in turn, stimulate proteolytic activation of caspase-3 (44). We show here that there is a substantial loss of $\Delta\Psi_m$ (Fig. 5*B*) and activation of caspase-3 (Fig. 5*C*) after KB cells are treated with BPR0L075. These results confirm that BPR0L075-induced apoptosis is associated with phosphorylation of Bcl-2, loss of $\Delta\Psi_m$, and activation of caspase-3.

Drug resistance is a common problem in the management of neoplastic disease, and the effectiveness of many clinically useful drugs is limited by the fact that they are substrates for the efflux pumps P-gp170/MDR and MRP. Notably, BPR0L075 *in vitro* was shown to be equally effective against three KB-derived MDR-positive cell lines (Table 1) via inhibition of tubulin polymerization despite P-gp170/MDR or MRP status (Fig. 2*C* and Fig. 3*A*); these findings suggest that BPR0L075 is a poor substrate of P-gp170/MDR and MRP. This feature is distinct from those of paclitaxel, vincristine, and colchicine because three KB-derived MDR-positive cells are much more resistant to these chemotherapeutic agents than KB cells. More importantly, BPR0L075 shows marked *in vivo* antitumoral activity in the KB, MKN-45, and P-gp170/MDR-overexpressing KB-VIN10 xenograft tumor models (Fig. 6*C*).

In conclusion, our data demonstrate that BPR0L075, a novel synthetic indole compound designed from CA-4, has properties distinct from colchicine, vincristine, and paclitaxel and is efficacious in suppressing cell growth in a variety of solid tumor models despite P-gp170/MDR or MRP status *in vitro* (45, 46). Furthermore, it exhibits significant antitumoral efficacy *in vivo*. These findings indicate BPR0L075 is a promising new tubulin-binding compound with potential for management of various malignancies, particularly for patients with demonstrated drug resistance.

ACKNOWLEDGMENTS

We thank Dr. Jacqueline Whang-Peng, Dr. Yu-Sheng Chao, Ms. Huey-Fang Wang, Ms. Hsiao-Wen Edith Chu, and Ms. Shiau-Fen Jung for their administrative support.

REFERENCES

1. Amos LA. Focusing-in on microtubules. Curr Opin Struct Biol 2000;10:236–41.
2. Margolis RL, Wilson L. Microtubule treadmilling: what goes around comes around. Bioessays 1998;20:830–6.
3. Wang LG, Liu XM, Kreis W, Budman DR. The effect of antimicrotubule agents on signal transduction pathways of apoptosis: a review. Cancer Chemother Pharmacol 1999;44:355–61.
4. Jordan A, Hadfield JA, Lawrence NJ, McGown AT. Tubulin as a target for anticancer drugs: agents which interact with the mitotic spindle. Med Res Rev 1998;18:259–96.
5. Shi Q, Chen K, Morris-Natschke SL, Lee KH. Recent progress in the development of tubulin inhibitors as antimitotic antitumor agents. Curr Pharm Des 1998;4:219–48.
6. Dumontet C, Sikic BI. Mechanisms of action of and resistance to antitubulin agents: microtubule dynamics, drug transport, and cell death. J Clin Oncol 1999;17:1061–70.
7. Deng L, Tatebe S, Lin-Lee YC, Ishikawa T, Kuo MT. MDR and MRP gene families as cellular determinant factors for resistance to clinical anticancer agents. Cancer Treat Res 2002;112:49–66.
8. Pettit GR, Singh SB, Boyd MR, et al. Antineoplastic agents. 291. Isolation and synthesis of combretastatins A-4, A-5, and A-6(1a). J Med Chem 1995;38:1666–72.
9. Gwaltney SL, Imade HM, Barr KJ, et al. Novel sulfonate analogues of combretastatin A-4: potent antimitotic agents. Bioorg Med Chem Lett 2001;11:871–4.
10. Dowlati A, Robertson K, Cooney M, et al. A phase I pharmacokinetic and translational study of the novel vascular targeting agent combretastatin a-4 phosphate on a single-dose intravenous schedule in patients with advanced cancer. Cancer Res 2002;62:3408–16.
11. Griggs J, Metcalfe JC, Hesketh R. Targeting tumour vasculature: the development of combretastatin A4. Lancet Oncol 2001;2:82–7.
12. Liou JP, Chang CW, Song JS, et al. Synthesis and structure-activity relationship of 2-aminobenzophenone derivatives as antimitotic agents. J Med Chem 2002;45:2556–62.
13. Nam NH. Combretastatin A-4 analogues as antimitotic antitumor agents. Curr Med Chem 2003;10:1697–722.
14. Gaj CL, Anyanwutaku I, Chang YH, Cheng YC. Decreased drug accumulation without increased drug efflux in a novel MRP-overexpressing multidrug-resistant cell line. Biochem Pharmacol 1998;55:1199–211.
15. Ferguson PJ, Fisher MH, Stephenson J, Li DH, Zhou BS, Cheng YC. Combined modalities of resistance in etoposide-resistant human KB cell lines. Cancer Res 1988;48:5956–64.
16. Finlay GJ, Baguley BC, Wilson WR. A semiautomated microculture method for investigating growth inhibitory effects of cytotoxic compounds on exponentially growing carcinoma cells. Anal Biochem 1984;139:272–7.
17. Tahir SK, Kovar P, Rosenberg SH, Ng SC. Rapid colchicine competition-binding scintillation proximity assay using biotin-labeled tubulin. Biotechniques 2000;29:156–60.
18. Tahir SK, Han EK, Credo B, et al. A-204197, a new tubulin-binding agent with antimitotic activity in tumor cell lines resistant to known microtubule inhibitors. Cancer Res 2001;61:5480–5.
19. Tahir SK, Nukkala MA, Zielinski Mozny NA, et al. Biological activity of A-289099: an orally active tubulin-binding indolyloxazoline derivative. Mol Cancer Ther 2003;2:227–33.
20. Cheng Y, Prusoff WH. Relationship between the inhibition constant (K1) and the concentration of inhibitor which causes 50 per cent inhibition (I50) of an enzymatic reaction. Biochem Pharmacol 1973;22:3099–108.
21. Bollag DM, McQueney PA, Zhu J, et al. Epothilones, a new class of microtubule-stabilizing agents with a taxol-like mechanism of action. Cancer Res 1995;55:2325–33.
22. Blagosklonny MV, Schulte TW, Nguyen P, Mimnaugh EG, Trepel J, Neckers L. Taxol induction of p21WAF1 and p53 requires c-raf-1. Cancer Res 1995;55:4623–6.
23. Jett JH. Mathematical analysis of DNA: histograms from asynchronous and synchronous cell populations. In: D. Lutz, editor. Pulse Cytophotometry. Brussels: European Press; 1978. p. 93–102.
24. Zamzami N, Metivier D, Kroemer G. Quantitation of mitochondrial transmembrane potential in cells and in isolated mitochondria. Methods Enzymol 2000;322:208–13.
25. Chen CT, Gan Y, Au JL, Wientjes MG. Androgen-dependent and -independent human prostate xenograft tumors as models for drug activity evaluation. Cancer Res 1998;58:2777–83.
26. Krajewski S, Tanaka S, Takayama S, Schibler MJ, Fenton W, Reed JC. Investigation of the subcellular distribution of the bcl-2 oncoprotein: residence in the nuclear envelope, endoplasmic reticulum, and outer mitochondrial membranes. Cancer Res 1993;53:4701–14.
27. Haldar S, Basu A, Croce CM. Bcl2 is the guardian of microtubule integrity. Cancer Res 1997;57:229–33.
28. Li P, Nijhawan D, Budihardjo I, et al. Cytochrome c and dATP-dependent formation of Apaf-1/caspase-9 complex initiates an apoptotic protease cascade. Cell 1997;91:479–89.
29. Cohen GM. Caspases: the executioners of apoptosis. Biochem J 1997;326:1–16.
30. Ben Sasson SA, Sherman Y, Gavrieli Y. Identification of dying cells in situ staining. Methods Cell Biol 1995;46:29–39.
31. King KL, Cidlowski JA. Cell cycle and apoptosis: common pathways to life and death. J Cell Biochem 1995;58:175–80.
32. Kumagai A, Dunphy WG. The cdc25 protein controls tyrosine dephosphorylation of the cdc2 protein in a cell-free system. Cell 1991;64:903–14.
33. Strausfeld U, Labbe JC, Fesquet D, et al. Dephosphorylation and activation of a p34cdc2/cyclin B complex in vitro by human CDC25 protein. Nature 1991;351:242–5.
34. Hoffmann I, Clarke PR, Marcote MJ, Karsenti E, Draetta G. Phosphorylation and activation of human cdc25-C by cdc2-cyclin B and its involvement in the self-amplification of MPF at mitosis. EMBO J 1993;12:53–63.
35. Sorger PK, Dobles M, Tournebize R, Hyman AA. Coupling cell division and cell death to microtubule dynamics. Curr Opin Cell Biol 1997;9:807–14.
36. Davis FM, Tsao TY, Fowler SK, Rao PN. Monoclonal antibodies to mitotic cells. Proc Natl Acad Sci USA 1983;80:2926–30.
37. Scatena CD, Stewart ZA, Mays D, et al. Mitotic phosphorylation of Bcl-2 during normal cell cycle progression and Taxol-induced growth arrest. J Biol Chem 1998;273:30777–84.
38. Blagosklonny MV, Giannakakou P, el Deiry WS, et al. Raf-1/bcl-2 phosphorylation: a step from microtubule damage to cell death. Cancer Res 1997;57:130–5.
39. Srivastava RK, Srivastava AR, Korsmeyer SJ, Nesterova M, Cho-Chung YS, Longo DL. Involvement of microtubules in the regulation of Bcl2 phosphorylation and apoptosis through cyclic AMP-dependent protein kinase. Mol Cell Biol 1998;18:3509–17.
40. Yamamoto K, Ichijo H, Korsmeyer SJ. BCL-2 is phosphorylated and inactivated by an ASK1/Jun N-terminal protein kinase pathway normally activated at G(2)/M. Mol Cell Biol 1999;19:8469–78.
41. Kluck RM, Bossy-Wetzel E, Green DR, Newmeyer DD. The release of cytochrome c from mitochondria: a primary site for Bcl-2 regulation of apoptosis. Science 1997;275:1132–6.
42. Marchetti P, Castedo M, Susin SA, et al. Mitochondrial permeability transition is a central coordinating event of apoptosis. J Exp Med 1996;184:1155–60.
43. Susin SA, Lorenzo HK, Zamzami N, et al. Mitochondrial release of caspase-2 and -9 during the apoptotic process. J Exp Med 1999;189:381–94.
44. Susin SA, Zamzami N, Castedo M, et al. The central executioner of apoptosis: multiple connections between protease activation and mitochondria in Fas/APO-1/CD95- and ceramide-induced apoptosis. J Exp Med 1997;186:25–37.
45. Beckers T, Reissmann T, Schmidt M, et al. 2-Aroylindoles, a novel class of potent, orally active small molecule tubulin inhibitors. Cancer Res 2002;62:3113–9.
46. Mahboobi S, Pongratz H, Hufsky H, et al. Synthetic 2-aroylindole derivatives as a new class of potent tubulin-inhibitory, antimitotic agents. J Med Chem 2001;44:4535–53.